The direction of local adaptation on pathogen exploitation rates reverses with environmental context

Elisa Visher[1,2], Anisha Ali[3,4], Jonathan Barajas[3], Sehar Masud[3], Annika McBride[3], Edwin Ramos[3], Melissa Sui[3,5], Cristina Villalobos-Heredia[3], Natalie Walzer[3], P. Signe White[1], Mike Boots[1,6]

1 Department of Integrative Biology, University of California, Berkeley, CA, 94720, USA

2 Department of Genetics, Stanford University, Stanford, CA, 94305, USA

3 University of California, Berkeley, CA, 94720, USA

4 Department of Psychology, Cal State East Bay, CA, 94542, USA

5 Department of Plant and Microbial Biology, University of California, Berkeley, CA, 94720, USA

6 5 College of Life and Environmental Sciences, University of Exeter, Penryn Campus, Penryn, TR10 9FE, UK

ABSTRACT

Host diversity and spatial heterogeneity are both predicted to impact parasite evolution, and these processes may interact in nature to impact local adaptation. Here, we experimentally evolve granulosis virus in microcosms of its *Plodia interpunctella* host with varied spatial structure and host genetic diversity. We find that virus evolves specific interactions with its locally familiar host genotype in both homogeneous and spatially heterogeneous host populations, but that the impact of local adaptation depends on the spatial structure. In one treatment, exploitation rates are higher on the familiar host, while, in the other, they are lower. While we find that food viscosity had unexpected impacts on the spatial structuring of contacts, spatially structured transmission may have led to the virus evolving more prudent exploitation rates on only the familiar host, leading to locally maladapted high exploitation rates on foreign hosts. Additionally, we also find that virus in heterogeneous microcosms is more locally adapted when there are higher contact rates between the hosts. Our experiment demonstrates that trade-offs optimizing exploitation rates at intermediate values, like those governing pathogen infectivity in spatial structure, may interact with trade-offs determining niche breadth in ways that can reverse the impact of local adaptation on pathogen phenotypes. [200/200]

INTRODUCTION

When trade-offs between different phenotypes act upon an organism, they can lead to a variety of evolutionary outcomes including the evolution of intermediate optimal strategies, evolutionary branching and niche partitioning, and cyclical dynamics [1–4]. Thus, trade-off theory underpins a wide array of ecological and evolutionary theory on adaptation and diversification [5,6]. One area where trade-offs are of particular importance is in explaining how biotic diversity is generated and maintained [7–9]. The idea here is that 'jacks-of-all-trades are the master of none', meaning that trade-offs between adaptation to different abiotic environments or biotic partners require an organism to choose between being a fit specialist or mediocre generalist [10]. For host-parasite interactions, this fundamental problem of niche breadth evolution becomes a question of host range evolution [11–13] and has implications for theories ranging from the Red queen hypothesis of sex [14,15], Janzen-Connell effects [16,17], Geographic mosaic theory [18], and zoonotic emergence [19,20].

However, it is an obvious fact that any organism is subject to multiple environmental pressures and thus a single phenotype may be simultaneously subject to multiple, potentially interacting trade-offs [21]. For example, while an organism's growth rates on different environments might trade-off with each other, that organism's growth rate might also be subject to life history trade-offs that select for intermediate optimal strategies [22]. Less appreciated is how the specific geometries and interactions between trade-offs can lead to different evolutionary outcomes for a system [22–25]. Depending on the order in which we consider our trade-offs in the above example, we could hypothesize that: 1) growth rates could be lower than maximal across the system, but still highest for the specialist on its familiar environment or 2) growth rates could be at the intermediate optimal level for both the specialist on its familiar environment and the 'mediocre' generalist on both. While the first type of interaction does mean that the outcome of evolution under multiple trade-offs is more consistent with the predictions of theory based on individual trade-offs and is thus more naturally assumed, there is no reason to expect that it should actually be more common. It is therefore necessary to better understand how trade-offs interact to determine how predictions of single trade-off theory scale into more ecologically realistic scenarios.

Here, we experimentally evolve granulosis virus in microcosms of its host *Plodia interpunctella,* the Indian meal moth (Hübner), host that vary in their host genetic diversity and spatial structuring. Altering host genetic diversity allows us to examine the consequences of trade-offs between host types on virus evolution [26], while altering the spatial structure of infectious contacts selects on pathogen exploitation rate [27]. Additionally, the spatial structuring of genetic diversity might further influence host range evolution due to differences in contact rates between hosts [28–30]. Thus, our experiment examines how pathogen evolves when experiencing a combination of selection pressures that are governed by separate, but potentially interacting, trade-offs.

On its own, spatially structured transmission is predicted to select for less infective, more prudent pathogens as higher proportions of local, rather than global, transmission mean that the pathogen competes with more closely related strains to deplete its local susceptible population and 'self-shade' [27,31–33]. Previous evolution experiments in the Plodia interpunctella and PiGV

system support this theory [34], as do experiments in microbial systems [35]. On its own, host heterogeneity is also predicted to select for less infective and virulent pathogens, but, in this case, the lower exploitation rates are due to evolutionary constraints where adapting to two host types mean that the pathogen is predicted to be less able to specialize on either one [8,26,36,37]. Some previous experiments in empirical systems confirm these hypotheses [38–43], but such constraints are not consistently observable and their exact nature is still unclear [37,44–48]. Our experiment therefore examines how an optimizing life history trade-off mediated by susceptible density and acting at the population level interacts with a constraint-based trade-off acting at the individual level.

Finally, the spatial structuring of host genetic diversity has important consequences for how pathogens are expected to evolve in metapopulations and locally adapt to different patches [49–51]. Theory suggests that contact rates between hosts, or migration between patches, should alter how pathogens are selected to specialize on their familiar host or become generalists. Higher contact rates between host types should select for generalists [28–30], but can also lead to greater local adaptation when migration increases the amount of genetic variation that selection can act upon and increases local competition for patches [52–54].

Our experiment therefore explores how trade-offs mediated by spatial structure and host heterogeneities interact and how the spatial structuring of host heterogeneity effects its impact on pathogen evolution. We find that manipulating the spatial structure of a population can reverse the impact of local adaptation on pathogen phenotypes so that they are less exploitative of their familiar host than of foreign hosts. We also find that virus in heterogeneous microcosms is more locally adapted when there are higher migration rates between the host types. These results imply that interactions between trade-offs mean that local adaptation might not always correlate with higher exploitation rates on the familiar host when optimizing life history trade-offs are simultaneously selecting for lowered exploitation rates.

METHODS

Study system

Plodia interpunctella, or the Indian meal moth, is a stored grain pest that naturally lives at high population density within its cereal food medium for 5 larval instar stages before it pupates into an adult moth that disperses, mates, and lays eggs, but does not eat [55,56]. It is naturally infected by the *Plodia interpunctella* granulosis virus (PiGV), a dsDNA baculovirus that transmits when larvae directly cannibalize infection killed cadavers or consume virus that was released into the environment from such cadavers [57,58]. Thus, the virus is an obligate killer that will only transmit if it kills its host. Notably, the virus can only infect *P. interpunctella* during the larval stages and, if exposed larvae clear the infection, they can pupate and carry out the rest of their life history as normal [59]. Infection killed cadavers are recognizable because successful infection turns larvae an opaque, chalky white color due to the high density of viral occlusion bodies [60]. The system has proved a powerful tool to examine the effects of spatial structure on pathogen exploitation rates and, more recently, host genotype specialization [34,61].

120 Host line selection and maintenance

121 For this experiment, we select 2 inbred populations of *P. interpunctella* that were previously
122 generated in the lab by brother-sister mating individuals for >27 generations [62]. Each
123 population should therefore be essentially a clonal population of two distinct host genotypes (Il-
124 9 and Il-17). These lines were chosen because they had similar levels of general resistance [61].
125 We have previously shown that virus evolved in homogeneous populations of these specific
126 inbred lines can specialize on its familiar host genotype by increasing their infectivity and/or
127 productivity [61].

128 We maintain these lines in wide mouthed Nalgene pots (ThermoFisher Scientific, U.K.) in the
129 absence of infection with 200g 'Standard' food medium (made in batches of 500g cereal mix (50%
130 Earth's Best oatmeal, 30% wheat bran, 20% rice flour), 100g brewer's yeast, 2.2g sorbic acid, 2.2g
131 methyl paraben, 125ml honey, and 125ml glycerol) in incubators set at 27±2 °C and 35±5%
132 humidity, with 16:8hr light: dark cycles [63]. To maintain populations, ~50 adult moths are moved
133 into a new pot with new food when they emerge monthly. Thus, host lines are maintained in the
134 absence of infection and do not evolve throughout the experiment.

135 Manipulating spatial structure

136 We manipulate spatial structure in the experiment by changing the viscosity of the food medium,
137 as in [34,64,65]. Because larvae live within their food medium, this alters individuals' dispersal
138 patterns and thus the spatial structure of their infectious contacts. We make food of two
139 viscosities, 'loose' and 'sticky', which differ solely in the amount of glycerol added. 'Loose' food
140 contains 500g Earth's Best oatmeal, 100g brewer's yeast, 2.2g sorbic acid, 2.2g methyl paraben,
141 and 175ml glycerol. 'Sticky' food contains 500g Earth's Best oatmeal, 100g brewer's yeast, 2.2g
142 sorbic acid, 2.2g methyl paraben, and 450ml glycerol. Food viscosity does not affect development
143 time or mass at pupation (Figure S1). 'Loose' and 'sticky' food is then added to wide-mouthed
144 Nalgene pots and frozen overnight to kill any insect eggs potentially contaminating the food. The
145 mass of food added to these pots (300g 'loose' and 550g 'sticky' food) was determined by the
146 volume needed to entirely fill half of one of our plastic microcosm containers.

147

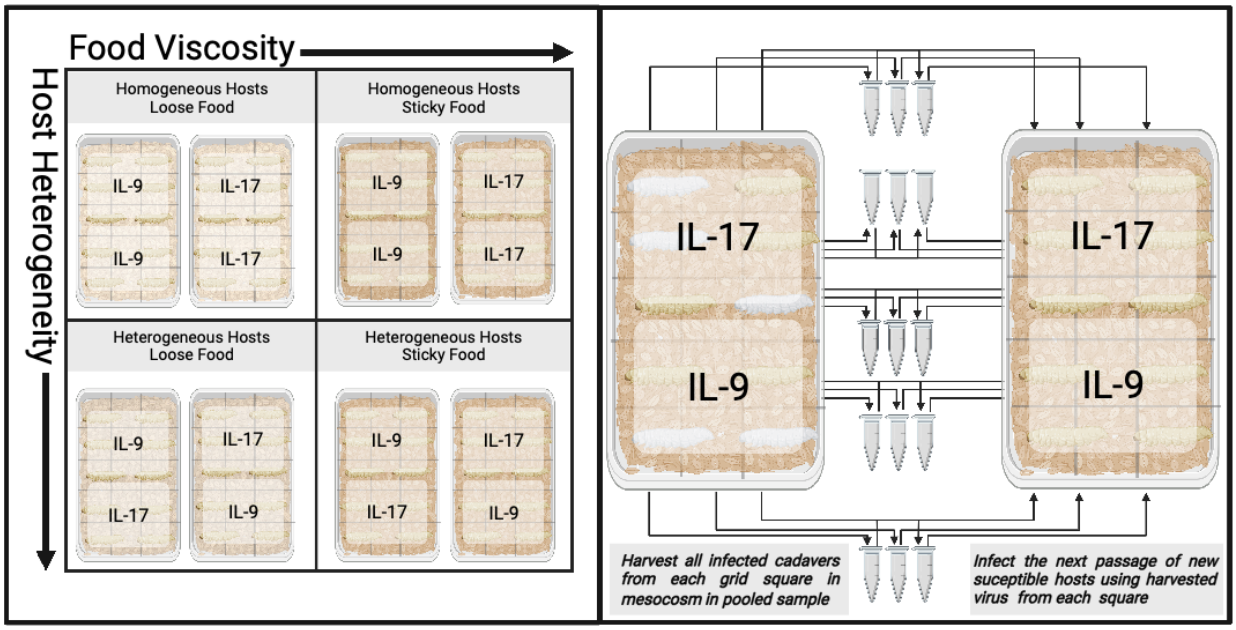

Figure 1: Experimental design and passaging scheme. (Left) Each microcosm is set up by adding 2 pots of food containing 11-day old larvae to opposite vertical ends of a plastic microcosm with a 3x5 grid. The 3rd row of the grid is therefore a contact zone between the sides. There are 3 replicates for each of the 8 microcosms. There are 4 different treatment types of homogeneous or heterogeneous hosts by 'loose' or 'sticky' food. Each homogeneous treatment is set up with both host types and each heterogeneous host treatment is set up alternating which host is on 'top' or 'bottom' of the grid. Microcosms are consistently oriented in the growth chamber so that the 'bottom' side is closer to the door. (Right) After 20 days incubating with virus, microcosms are frozen and dissected into grid squares. All infected larvae from each grid square are harvested and added to a 1.5mL Eppendorf tube (1 square per tube) and homogenized to release occlusion bodies. 500mL of the virus solution is then pipetted in droplets over the same grid square of a new microcosm of the same treatment set-up with fresh 11-day old hosts. Therefore, the spatial force of infection is preserved across passages. We experimentally evolve virus for 10 passages.

<u>Setting up host populations for microcosms</u>

After thawing the pots of 'sticky' and 'loose' food, we add ~50 similarly aged adult moths to each pot from either our Il-9 or Il-17 host maintenance populations and incubate them for 10 days as in Figure 1. These single-genotype adults mate and lay eggs into the 'sticky' or 'loose' food. 10 days after adding adults, these pots containing Il-17 larvae in 'loose food, Il-17 larvae in 'sticky' food, Il-9 larvae in 'loose' food, or Il-9 larvae in 'sticky' food are used to set up microcosms. Therefore, pots are set up with the same number of adults, but may not contain the same number of larvae.

Microcosms are set up in 9.25" x 12.08" x 0.9" inch plastic A4 document cases (Daiso Japan, U.S.A.) that have been marked with an even 3 x 5 grid of 3.08" x 2.42" squares. We set up 8 microcosms per replicate: 1) homogeneous Il-9 hosts in 'loose' food; 2) homogeneous Il-17 hosts in 'loose' food; 3) homogeneous Il-9 hosts in 'sticky' food; 4) homogeneous Il-17 hosts in 'sticky' food; 5) heterogeneous hosts (Il-9 on top / Il-17 on bottom) in 'loose' food; 6) heterogeneous hosts (Il-17 on top / Il-9 on bottom) in 'loose' food; 7) heterogeneous hosts (Il-17 on top / Il-9 on bottom) in 'sticky' food ; and 8) 7) heterogeneous hosts (Il-9 on top / Il-17 on bottom) in 'sticky' food (Figure 1). Each microcosm therefore has a single food type (either 'sticky' or 'loose'),

177 according to its treatment. To arrange hosts in the microcosm, we add 2 pots of the food
178 containing 10-day old larvae to opposite vertical ends of the grid, so that food fully fills the plastic
179 containers. For homogeneous host treatments, we add 2 pots containing larvae of the same
180 genotype (either both Il-9 or both Il-17) and, for heterogeneous treatments, these 2 pots contain
181 larvae of different genotypes. Thus, homogeneous genotype microcosms have a single genotype
182 of host throughout the grid, while heterogeneous microcosms have two genotypes separated
183 vertically across the grid with a contact zone at the 3rd row. To balance our treatments and
184 account for potential effects due to position within the grid, we set up 2 microcosms of each of
185 the 2 heterogeneous treatments and alternate which genotype is on 'top'. There are therefore 8
186 unique microcosm types.

187 These microcosms are then incubated overnight, as above, so that virus can be added to them
188 on day 11. We repeat this process each passage to set up new microcosms so that evolving virus
189 can be added to a fresh microcosm. This allows us to maintain 2 non-interbreeding and non-
190 evolving host genotypes in our microcosms and preserve the spatial structuring of such
191 genotypes across passages.

192 Experimental evolution

193 We set up 3 replicates of each of our 8 unique microcosm types (24 serially passaged microcosms
194 total). Experimental evolution is initiated by pipetting 5ml of 10^{-2} stock virus solution in small
195 droplets evenly over the top of each microcosm. Each microcosm is then incubated for 20 days
196 and then frozen overnight to kill larvae for harvesting. Passage lengths (10 days before set-up, 1
197 day overnight, 20 days with virus) therefore roughly correspond to the host's natural ~monthly
198 cyclical demography [65]. We stagger the replicates' passaging schedules weekly due to the time
199 intensive nature of passaging.

200 To harvest virus, we dissect each microcosm by grid square and separately collect infection killed
201 cadavers from each square in sterile 1.5ml Eppendorf tubes (Figure 1). We add 1ml sterile, MilliQ
202 water to each square's tube and use a sterile pellet pestle (Fisher Scientific, U.S.A.) to manually
203 burst larvae and release viral occlusion bodies. We droplet 500ul of this solution from each
204 square onto the same square of that treatment's freshly set-up microcosm to infect the next
205 passage and freeze the rest of the solution. Therefore, we preserved the force of and spatial
206 structure of infection within the grid across passages. We record the number of infected cadavers
207 in each square at each passage to track the spatial ecology of infection in the experiment.

208 The microcosms newly infected with passaged virus were then placed back into incubators for 20
209 days to allow the virus to infect larvae for the next passage. We experimentally evolve virus for
210 10 passages, a number standard for microbial evolution experiments. There are several occasions
211 where we had to use the frozen virus solutions reserved during passaging to re-set up passages
212 due to low numbers of infected cadavers or contamination with another pathogen.
213 Contamination was recognizable because the most common contaminant, *Bacillus thuringiensis*
214 (Bt), turns infected larvae black rather than white [66]. We could generally expect any co-infected
215 larvae to display the black phenotype since Bt kills larvae more quickly (Yitbarak, unpublished
216 data), so re-setting up passages when Bt was visually detected would clear the virus population.
217 Congruously, we did not see any signs of persistent contamination within our passages nor in any
218 of our assays.

219 Assay

220 After passage 10, we collect and virus infected cadavers from each square as above. We next
221 pool the virus from the 3 squares in each row of the 3x5 grid in equal proportion so that we have
222 5 virus samples per microcosm. Each pooled sample is therefore the virus population at a certain
223 vertical position within the microcosm, along the gradient of heterogeneity for the
224 heterogeneous host microcosms. We purify virus by centrifuging for 1 min at 3000 rpm to remove
225 larger particulate matter and then 3 min at 13000 rpm to pellet virus. We run these samples
226 through a .65 micron filter to semi-purify our virus of larger bacterial and fungal contaminants,
227 as in [61]. Next, we quantify the concentrations of each sample by counting occlusion bodies on
228 a Petroff-Hauser counting chamber with 400x darkfield microscopy and dilute each to an assay
229 dose concentration of ~7.5x10^8 occlusion bodies per mL in 2% sucrose and .2% dye [61]. The
230 sugar entices the larvae to ingest the virus and the dye allows the experimenter to determine
231 which have ingested half their body lengths of solution and are considered exposed.

232 We assay each pooled virus sample on both of our 2 host genotypes, Il-9 and Il-17, to determine
233 the proportion of hosts each virus sample infects on each genotype and the average number of
234 occlusion bodies each virus sample produces per infection on each genotype. With 5 virus
235 samples for each of the 8 microcosms that have 3 replicates, this results in 240 virus sample x
236 assay line combinations. We batch these assays to infect 1 genotype with all 5 virus samples for
237 4 of the microcosms of 1 replicate each day. Since we can only assay half of a replicate's
238 microcosms each day, we balance the batches so that the 4 microcosms assayed each day have
239 equal homogeneity/heterogeneity, Il-9/Il-17 proportions, and loose/sticky food. Because only 1
240 assay genotype is assayed per day, we include assay genotype in all statistical models to account
241 both for general differences in resistance and assay day effects.

242 To set up infectivity assays, we first move ~70-80 adult moths of the appropriate inbred line for
243 the batch into new pots with 200g 'standard' food. Eleven days after setting up assay pots, we
244 collect 100 third instar larvae for each assay combination in a petri dish and stave them under a
245 damp paper towel for 2 hours. After starvation, we syringe tiny droplets of the appropriate virus-
246 sucrose-dye solution onto the petri dish for the larvae to consume. We add 50 larvae that have
247 orally ingested half their body lengths of virus solution to 2 25-cell compartmentalized square
248 petri dishes (ThermoFisher Scientific, U.S.A.) with 'standard' food and incubate them for 20 days
249 [61]. Assay grids are labelled with random identifiers to blind assay combinations and prevent
250 bias. After 20 days, assay grids are frozen and destructively sampled to count the number of
251 infected and uninfected individuals in each grid. Infected cadavers from each assay grid are then
252 saved in a pooled sample for virus quantification.

253 To determine the average number of occlusion bodies produced per infected individual, we
254 extract virus from the pooled samples from each assay grid using a sterile pellet pestle (Fisher
255 Scientific, U.S.A.) to manually burst larvae and release viral occlusion bodies. We then centrifuge
256 these samples as above, but do not filter them, and count occlusion bodies on the Petroff-Hauser
257 counting chamber. The concentration of occlusion bodies is then divided by the number of
258 infected cadavers that were in the pooled sample to get the average number of occlusion bodies
259 produced per infection for each virus sample on each host genotype.

260 Statistical analyses

261 We analyze our data using a generalized linear mixed modelling framework in R [67]. All models
262 were run in R version 4.2.3 (2023-03-15) -- "Shortstop Beagle" [68]. We used packages
263 'glmmTMB' and 'lme4' to build models, 'DHARMa' to check model residuals, 'afex' and 'car' to
264 determine significant model terms, 'emmeans' to extract effects, 'tidyverse' to manipulate data,
265 and 'patchwork' and 'ggplot2' to plot results [69–77]. We determine error structures for models
266 by testing fitted models with 'DHARMa' and then adjusting to best fit residuals. On occasion,
267 observation level random effects are used to correct overdispersion in our models [78]. Where
268 necessary, contrasts are used with 'emmeans' to determine effect estimates for treatments. All
269 model tables and annotated code are in the supplement.

270 Infection time series analysis

271 We examine the spatial structuring of transmission using the data collected on the number of
272 infected individuals in each square at each passage for each microcosm. To determine whether
273 food viscosity affected the spatial structuring of infection, we built a generalized linear mixed
274 model (GLMM) with a negative binomial distribution ('nbinom1') that asked whether the number
275 of infected individuals in a square is significantly predicted by the number of infected individuals
276 in that same square at the previous passage and whether this term interacted with food viscosity.
277 The model also included a fixed effect of the position of the square itself (to account for larval
278 preferences in where they moved) and random effects of passage number, replicate, the pot of
279 larvae used to set up that half of the microcosm (to roughly account for susceptible density), and
280 observation ID.

281 We additionally run a Levene's Test for Homogeneity of Variance on the infected count data to
282 determine if our 'sticky' and 'loose' food treatments differ in their variance, a measure of how
283 'clumpy' infection is within a microcosm.

284 Assay analysis

285 Infectivity and productivity assay data was analyzed in a generalized linear mixed modeling
286 framework using the same packages and process as above [67]. We build models treating
287 proportion infected, average number of occlusion bodies per infected individual, and the
288 composite exploitation rate (proportion infected multiplied by the average occlusion body count)
289 as our response variables. We transform average virus counts and composite exploitation rates
290 by multiplying and rounding them to produce integer counts for Poisson and negative binomial
291 distribution assumptions. In each model, we include random effects for batch and the nested
292 effect of virus sample under replicate under treatment.

293 First, we ask whether virus populations significantly differ in their specialization at the whole
294 microcosm level by building models that include an interaction effect between the assay being
295 on the host that the population was evolved on ('familiar') or the foreign host and the type of
296 food the population evolved in. Virus from heterogeneous populations is coded as
297 'heterogenous' as they do not have a familiar or foreign host at the whole microcosm level. We
298 also include assay line as a fixed effect to account for overall differences in resistance between
299 our assay host genotypes. The infectivity model uses a binomial error structure with observation
300 level random effects, the productivity model uses a Poisson error structure with observation level
301 random effects, and the exploitation rate model uses a zero-inflated negative binomial error

302 structure with observation level random effects. To better see the effects of specialization in the
303 homogeneous populations, we also run these same models for the homogeneous host
304 treatments only with the infectivity model using a binomial error structure, the productivity
305 model using a Poisson error structure, and the exploitation rate model using a negative binomial
306 error structure with observation level random effects.

307 Next, we ask whether spatial structure or host heterogeneity have significant effects on viral
308 phenotypes across genotypes (without accounting an effect of local adaptation). We build
309 models for infectivity and productivity with the same random effects as above, and without fixed
310 effects for being assayed on the familiar or foreign host. For host heterogeneity models, we
311 include the assay line, food type, and whether the treatment had homogeneous or
312 heterogeneous hosts as fixed effects, allowing for an interaction between food type and
313 treatment heterogeneity. The infectivity model uses a binomial error structure with observation
314 level random effects and the productivity and composite exploitation models use a zero-inflated
315 negative binomial error structure with observation level random effects. For spatial structure
316 models, we include the food type and assay line as fixed effects with the same random effects as
317 above. The infectivity model uses a binomial error structure, and the productivity and composite
318 exploitation models use a zero inflated negative binomial structure with observation level
319 random effects.

320 Finally, we ask whether virus phenotypes are spatially structured within the heterogeneous host
321 treatments. First, the local proportion of host genotype 17 is determined for each virus
322 population by its distance from the host contact zone so that the edge of the microcosm where
323 host genotype 17 was added is coded as 1, the next row of the grid is coded .75, the middle
324 contact zone is coded as 0.5, the following row is coded as .25, and the edge of the microcosm
325 where host genotype 9 was added is coded as 0. We build models for infectivity, productivity,
326 and exploitation rate that include the local proportion of host genotype 17, the host genotype of
327 the assay, the food type, and interaction effects between all three fixed terms. We include the
328 same random effects as in the previous models for batch and nestedness, but also include
329 random terms for the specific position and order of lines to account for the fact that we have two
330 heterogeneity treatments that differ in which line is on 'top' or 'bottom' of the microcosm. The
331 infectivity model uses a binomial error structure, the productivity model uses a Poisson error
332 structure with observation level random effects, and the exploitation rate model uses a zero-
333 inflated negative binomial error structure.

334

335 **RESULTS**

336 <u>Food viscosity spatially structures of infection</u>

337 Across the whole experiment, the density of infected hosts in a position positively correlates with
338 the density of infected hosts in that position in the previous passage (Figure 2, estimate = 0.009,
339 $p = 0.011$). There are also significant effects of the position itself ($p < 0.001$), where infection is
340 more likely to be found in corner and edge squares of the microcosm and on the side closer to
341 light, and the type of food, where infection is higher in 'sticky' food (estimate = 0.26, $p < 0.001$).
342 Importantly, there is a significant interaction term between the effect of infected density at a

343 position in the previous passage and the type of food (p=.043). However, the predictive power
344 of the previous passage's density of infected hosts in a position is significantly weaker for 'sticky'
345 food that for 'loose' food (Figure 2, estimate = -0.009, p = 0.043). This means that, contrary to
346 our expectations, 'loose' food spatially structures infection at the grid square level more than
347 'sticky' food in our experiment. From experimenter observation, it seems likely that this is
348 because 'loose' food packed microcosms more precisely than 'sticky' food, leaving fewer gaps for
349 larvae to exit the food into and move unimpeded along. At the same time, however, the food
350 types also differ in the variance of their infected count data (p < 0.001), with 'sticky' food having
351 more clustered infected individuals (Figure S2).

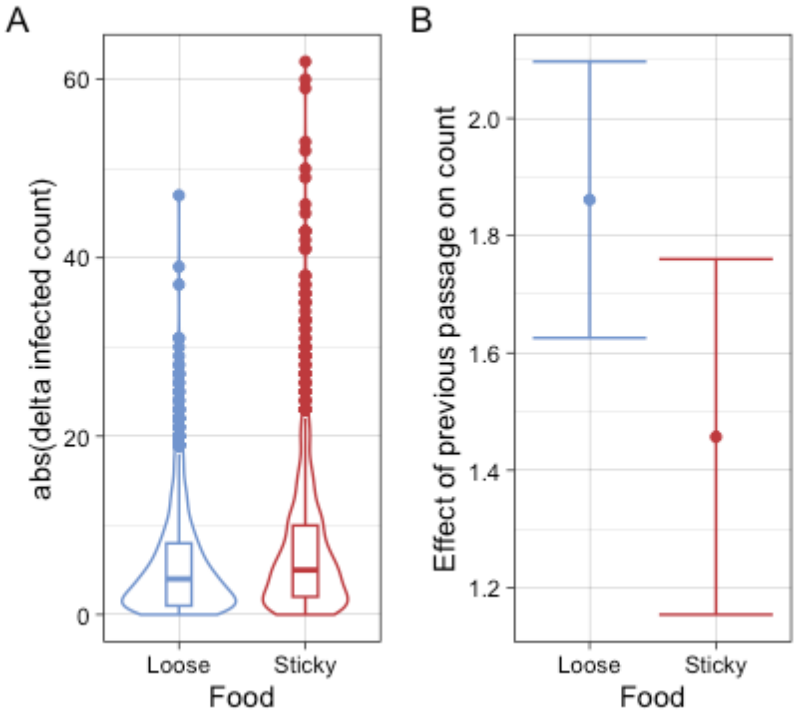

352

353 *Figure 2: (A) Change in the number of infected cadavers in a square between passages (y-axis) for 'loose' and 'sticky'*
354 *food (x-axis). (B) Effect estimates drawn from a GLMM for the interaction between type of food evolved on and the*
355 *effect of the previous passage's infection count at a square on the current passage's infected count on a square.*

356

357 <u>The impact of local adaptation on virus phenotypes depends on spatial structure</u>

358 Averaged across host genotypes, the spatial structure manipulation does not affect virus
359 populations evolved per particle infectivity (p = 0.96) or per infection virus productivity (p = 0.58)
360 (Figure S4). This is in contrast to previous results that only assay virus on genetically diverse local
361 hosts [34]. However, any impact of spatial structure may also depend on local adaptation as
362 evolved virus populations are assayed on both familiar and foreign hosts. When we test whether
363 spatial structure interacts with host genotype specialization, we find that there are significant
364 interaction effects between which host genotype the population was evolved on, the host
365 genotype assayed on, and the type of food evolved on (Figure 3). Specifically, for virus
366 populations evolved in homogeneous host populations, viruses from 'loose' food populations are

less infective on their familiar host (estimate = -0.785, p = 0.031) while those from 'sticky' food populations do not significantly differ in infectivity between familiar and foreign hosts (estimate = 0.442, p = 0.22) (Figure 3B). Simultaneously, viruses from 'loose' food populations are less productive on their familiar host (estimate = -0.451, p =.032) while those from 'sticky' food are significantly more productive on familiar hosts (estimate = 0.198, p =0.347) (Figure 3D). Collectively, this means that the effect of being assayed on a familiar or foreign host significantly (p=0.047) depends on food type so that the viruses are more prudent on their familiar hosts in 'loose' food and more exploitative on familiar hosts in 'sticky' food (loose estimate=-1.29 p=0.037; sticky estimate=1.02, p=0.09) (Figure 3F).

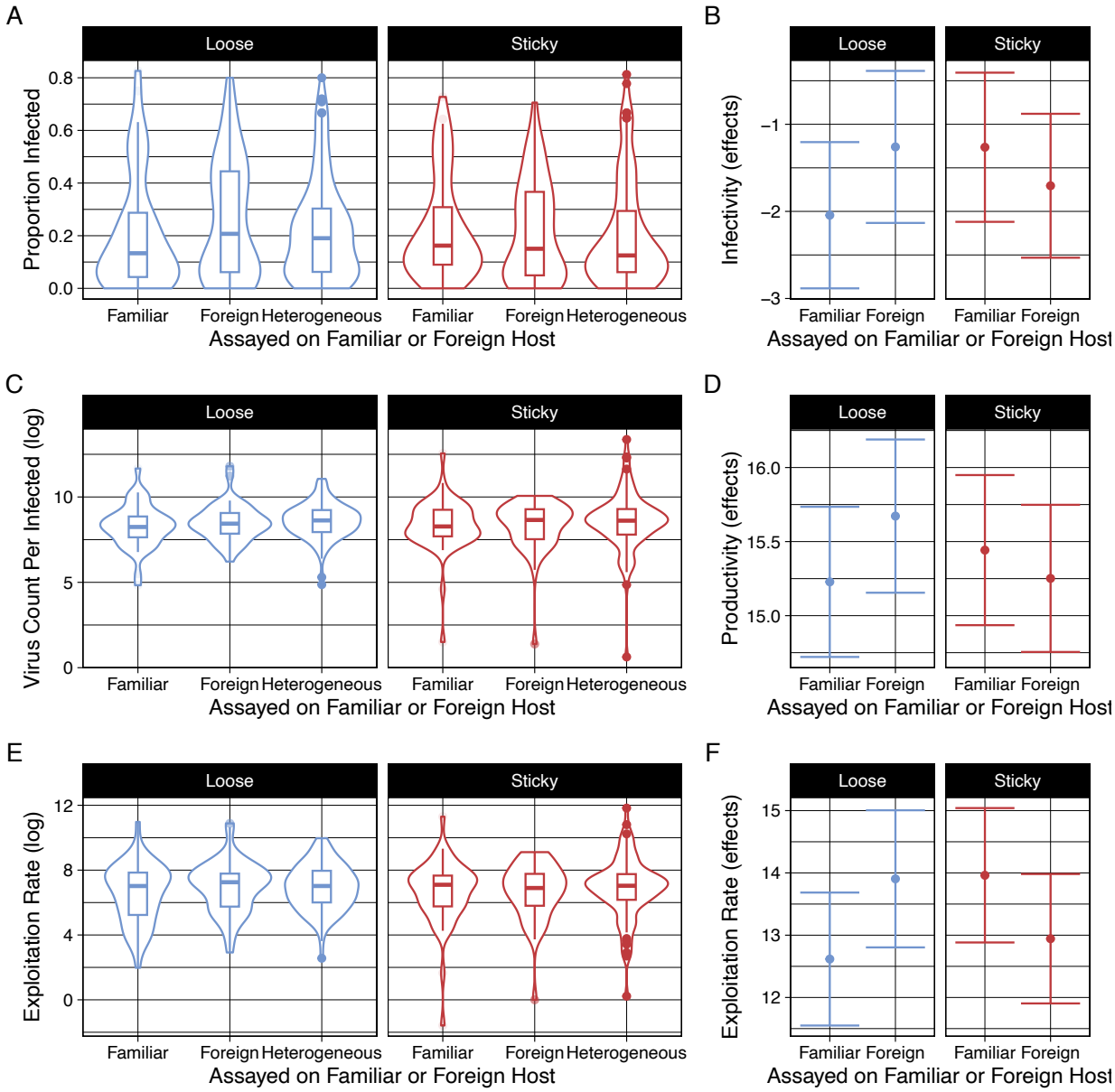

Figure 3: Interactions between local adaptation and the spatial structuring of infection. Panels A, C, E plot raw data and panels B, D, F show model effect estimates drawn from GLMMs for the homogeneous host dataset. Y-axes

*represent: (A) proportion infected, (B) effect estimates for the infectivity model for homogeneous host treatments only, (C) average number of occlusion bodies produced per infectious cadaver on a log scale, (D) effect estimates for the viral productivity model for homogeneous host treatments only, (E) composite exploitation rate (proportion infected * average number of occlusion bodies) on a log scale, and (F) effect estimates for the exploitation rate model for homogeneous host treatments only. X-axes represent whether the virus from homogeneous host treatments was being assayed on the host genotype that it evolved on or on the foreign host genotype (A-F) or whether the virus came from a heterogeneous host treatment (A, C, E). Panels show whether the virus came from a treatment with 'loose' food or 'sticky' food.*

Spatially structured host genetic diversity leads to local adaptation

On average, virus populations evolved in heterogeneous host populations do not significantly differ in infectivity (p = 0.60) or composite exploitation (p=0.20) from those evolved in homogeneous host populations, though they are slightly more productive (estimate=0.14, p=0.42). However, heterogeneous host populations have gradients of host mixing within them as the different positions are different distances from the other host genotype. Additionally, we expect spatial structure to impede host movement and thus further alter the degree of host mixing for different positions. Therefore, we explore whether there is an effect host specialization within the heterogeneous host microcosms and whether this effect is altered by the spatial structuring of the population. We find that there is a significant interaction between the local proportion of a host genotype (i.e., the position's distance from the contact zone) and the bias in exploitation rate (a composite metric of virus infectivity and productivity) that is mediated by the type of food evolved in (p = 0.031, Figure 4). As in homogeneous populations, virus populations are biased towards higher exploitation rates on familiar hosts in 'sticky' food populations (estimate=1.714, p=0.03) and somewhat lower exploitation rates on familiar hosts in 'loose' food populations (estimate=-0.604, p =0.40).

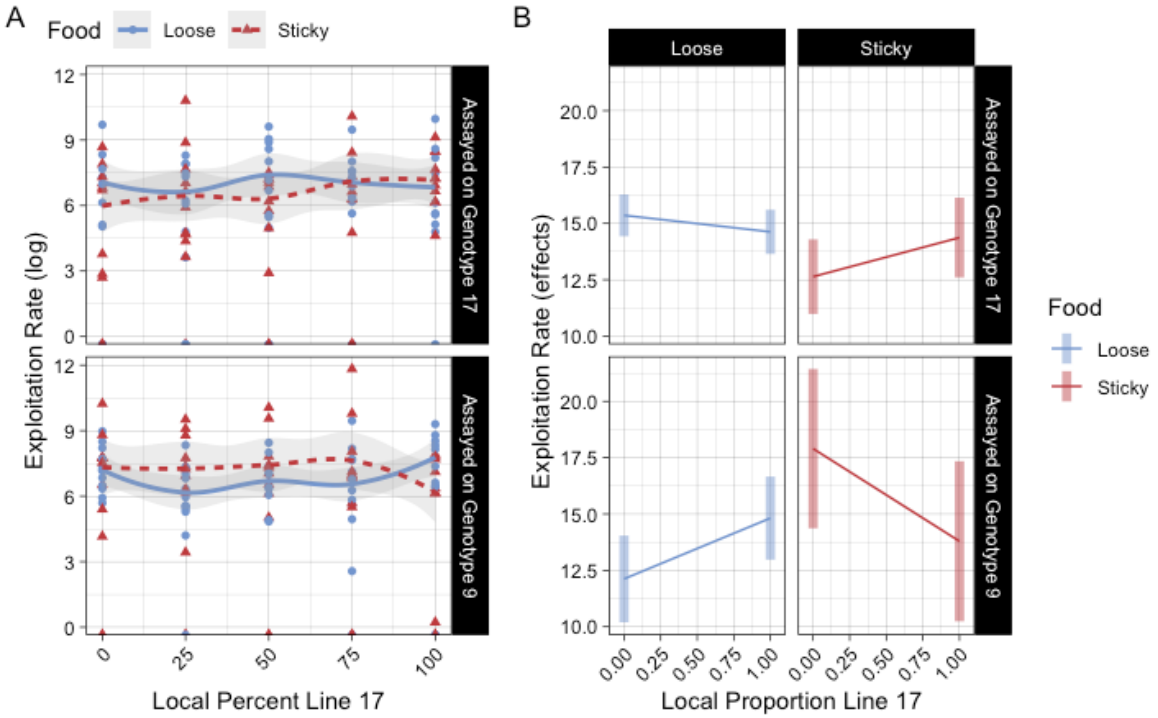

*Figure 4: Interactions between local adaptation and the spatial structuring of infection within heterogeneous host populations. (A) Raw data for the composite exploitation rate (proportion infected * average number of occlusion bodies, log-scale, y-axis) for virus sampled from different spatial positions within the microcosm with different degrees of mixing between the 2 host types (x-axis). Virus from 'loose' food treatments is represented with circle points and solid line and virus from 'sticky' food treatments is represented with triangle points and dashed line. Panels represent which host genotype the virus was assayed on. (B) Model effect estimates drawn from a GLMM for the effects of food type and assay genotype on exploitation rate (y-axis) for virus sampled from different spatial positions within the microcosm with different degrees of mixing between the 2 host types (x-axis). Panels are separated horizontally by food type and vertically by which host genotype the virus was assayed on.*

DISCUSSION

In our experiment, we find that pathogens can evolve to be more exploitative of their familiar host on one food type and less exploitative of their familiar host on the other food type. This effect holds at both the treatment level for virus lines evolved in homogeneous host environments and as a gradient affect in heterogeneous host environments where the degree of local adaptation depends on the distance from the host contact zone (Figure 3, Figure 4). Therefore, our experiment suggests that the multiple selection pressures (host genetic diversity and spatial structure) that our virus populations experience led to their host range and life history trade-offs interacting and reversing the outcome of local adaption on pathogen exploitation rate. This has important implications for eco-evolutionary theory.

A large portion of ecological and evolutionary theory on how host-parasite coevolution can result in biotic diversity depends on specialist interactions and assumes that pathogens have the highest exploitation rates on their familiar or locally common host so that rare hosts have a fitness advantage [6,15,79,80]. This is partially because most of these models focus only on the infectivity component of pathogen specialization and do not consider post-infection processes

429 like replication and virulence where high levels might be expected to lower fitness [81]. However,
430 our results suggest that infectivity might also not always be higher on the familiar host when
431 more prudent strategies are fitter [82].

432 The implications of certain ecological and population structures leading to maladaptively higher
433 exploitation rates on foreign, or rare, hosts have not previously been extensively considered.
434 When transmission between host types is low, maladaptively high virulence on a host would lead
435 to stuttering transmission chains and local extirpation of the pathogen in the rare host and
436 preserve rare genotype advantage [19,83]. However, when transmission between host types
437 freely occurs, selection for lower exploitation rates on the familiar host resulting in maladaptively
438 high exploitation on foreign or rare hosts means that rare genotype advantage is not ubiquitous
439 [81]. This has previously been considered in cases of species invasions (i.e. 'invading with
440 weapons') and zoonosis [84,85], but not for host-parasite coevolutionary theory at equilibrium.
441 Therefore, environments selecting for lower exploitation rates may also be less likely to conform
442 to the predictions of eco-evolutionary theory that depends on this rare genotype advantage like
443 the Red Queen Hypothesis of Sex [14] and Janzen-Connell effects [16,17]. Additionally, we should
444 not always expect pathogens to have the highest exploitation rates on their familiar host, even
445 in the absence of co-evolutionary dynamics where the host might be further 'ahead' in the arms
446 race [86]. Our data shows that patterns approximating the host being 'ahead' in a coevolutionary
447 arms race can be found even in the absence of host evolution.

448 Our result that virus evolves lower exploitation rates on the familiar host in one of our food types
449 could be understood if food viscosity was spatially structuring infectious contacts so that
450 pathogens were selected to lower their exploitation rates, but that they were only selected to do
451 so on the familiar host. While the pathogen would be selected to have the highest fitness on its
452 familiar host in each treatment, the optimal exploitation rate associated with that peak fitness
453 would depend on the spatial structuring of infectious contacts (because self-shading in spatial
454 structured environments selects for more prudent pathogen strategies) [33]. This means that the
455 pathogens selected in spatially structured environments could actually have higher exploitation
456 rates on foreign host genotypes than familiar.

457 However, our evolution experiment resulted in lower exploitation rates on the familiar host in
458 'loose' food, despite our expectations that 'sticky' food would spatially structure the population
459 more. Previous experiments with similar food types used 'sticky' food to spatially populations as
460 they, and our preliminary experiments, showed that 'sticky' food impedes larval movement
461 (Table S1) [34,64]. Therefore, we were expecting to see lowered exploitation rates in 'sticky' food,
462 rather than 'loose' food. However, we do have evidence that our food viscosity manipulation
463 behaved in unexpected ways. Our infection ecology data seems to suggest that 'loose' food
464 spatially structured infection more than 'sticky' food at the level of force of infection within a
465 3.08" x 2.42" grid square between passages. One reason for the different outcome in our
466 experiment may be that slight differences in 'sticky' food viscosity can lead to higher rates of
467 larvae exiting the food to move unimpeded along the surface. While we added enough food to
468 entirely fill our plastic microcosms, the 'sticky' food was clumpier and left more air gaps on the
469 surface of the food than the 'loose' food. Therefore, larvae in 'sticky' food may have been more
470 likely to travel between grid squares along the surface of the food so that infection was more
471 spatially structured in 'loose' food treatments. Alternatively, it is possible that the virus had

472 different rates of environmental decay on the different food types leading to differences in where
473 larvae were infected. Another potential explanation is that eggs and early instar larvae may have
474 been more 'clumped' in 'sticky' food so that the density of susceptible individuals was more
475 heterogeneous and influenced the local infection density more than the dose of virus added to
476 the square. The fact that 'sticky' food microcosms are more heterogeneous in the clustering of
477 infected individuals potentially supports this interpretation. Therefore, the infection ecology
478 results suggest that 'loose' food spatially structured infection more than 'sticky' food at the grid
479 square level between passages, but we have no way of determining how food structured
480 infection at the sub-square level, when larvae were earlier instar with lower movement rates. It
481 is possible that 'sticky' food less structured infection between passages at the square spatial
482 scale, but structured contacts at smaller spatial scales early in each passage.

483 However, greater spatial structuring of infectious contacts in the 'loose' food would provide a
484 plausible mechanism for why lower exploitation rates evolved on the familiar host in these lines.
485 It is difficult to think of another plausible hypothesis. As force of infection was higher during
486 passaging in the 'sticky' food lines, it is possible that 'sticky' lines had stronger selection to
487 specialize on the familiar host, but this could explain why effect sizes of specialization could vary,
488 but not why they would switch directions [87]. Alternatively, it is plausible that infection in 'sticky'
489 food infected earlier instar larvae as the high numbers of infected individuals in certain squares
490 during selection passages were observationally correlated with clusters of early instar larvae and
491 'sticky' food moderately slows development (Figure S1). However, we would expect this to lead
492 to lower exploitation rates on the familiar host in 'sticky' food as earlier instar larvae are both
493 less resistant and, potentially, more spatially structured [88]. Therefore, the most likely
494 hypothesis to explain these results seems to be that the higher spatial structuring of spatial
495 contacts at the grid-square level between passages in the 'loose' food imposed a spatial
496 structuring effect that selected for lower exploitation rates on the familiar host.

497 Another key, but slightly counterintuitive, result of our experiment is that the effects of local
498 adaptation in heterogeneous host environments are stronger in better mixed populations than
499 in more spatially structured ones (Figure 4). As host genotype mixing only depends on spatial
500 structure effects above the square scale, we can better assume that 'loose' food more strongly
501 structured contacts between genotypes than 'sticky' food. While more contact between host
502 genotypes should, in theory, select more strongly for generalism [28–30], theory suggests that
503 higher migration rates between patches can lead to stronger local adaptation due to migration
504 conferring more genetic diversity to select from and increased competition to strengthen such
505 selection [54]. Our experiment seems to support the latter theory, implying that certain rates of
506 migration between populations may support, rather than homogenize, phenotypic diversity.

507 Our ability to make conclusions is hampered by the fact that our experimental manipulation for
508 spatial structure seemed to have worked in the opposite direction as intended. However, our
509 results do suggest that evolution in response to multiple selection pressures can be governed by
510 interacting trade-offs and result in different locally adapted optimal strategies. Specifically, when
511 optimal exploitation strategies on the familiar host are more prudent, pathogens may have
512 maladaptively high exploitation rates on foreign hosts. Furthermore, our experiment shows that
513 higher pathogen migration rates between host types can lead to stronger effects of local
514 adaptation, suggesting that some population mixing might support metapopulation diversity.

Our result that interactions with other trade-offs can reverse the impact of local adaptation on pathogen exploitation rate has important implications for eco-evolutionary theory on the maintenance of diversity that depends on rare genotype advantage.

REFERENCES

1. Ackermann M, Doebeli M. 2004 Evolution of Niche Width and Adaptive Diversification. *Evolution* **58**, 2599–2612. (doi:10.1111/j.0014-3820.2004.tb01614.x)

2. Dieckmann U, Marrow P, Law R. 1995 Evolutionary cycling in predator-prey interactions: population dynamics and the red queen. *J. Theor. Biol.* **176**, 91–102. (doi:10.1006/jtbi.1995.0179)

3. Farahpour F, Saeedghalati M, Brauer VS, Hoffmann D. 2018 Trade-off shapes diversity in eco-evolutionary dynamics. *eLife* **7**, e36273. (doi:10.7554/eLife.36273)

4. Geritz SAH, Kisdi E, Mesze´NA G, Metz JAJ. 1998 Evolutionarily singular strategies and the adaptive growth and branching of the evolutionary tree. *Evol. Ecol.* **12**, 35–57. (doi:10.1023/A:1006554906681)

5. Agrawal AA, Conner JK, Rasmann S. 2010 Tradeoffs and Negative Correlations in Evolutionary Ecology. In *Evolution since Darwin: the first*, pp. 243–268.

6. Chesson P. 2000 Mechanisms of Maintenance of Species Diversity. *Annu. Rev. Ecol. Syst.* **31**, 343–366. (doi:10.1146/annurev.ecolsys.31.1.343)

7. Godsoe W, Bellingham P, Moltchanova E. 2021 Disentangling niche theory and beta diversity change. *Am. Nat.* (doi:10.1086/718592)

8. Levins R. 1962 Theory of Fitness in a Heterogeneous Environment. I. The Fitness Set and Adaptive Function. *Am. Nat.* **96**, 361–373. (doi:10.1086/282245)

9. Macarthur R, Levins R. 1967 The Limiting Similarity, Convergence, and Divergence of Coexisting Species. *Am. Nat.* **101**, 377–385. (doi:10.1086/282505)

10. MacArthur RH. 1984 *Geographical Ecology: Patterns in the Distribution of Species*. Princeton University Press.

11. Antonovics J, Boots M, Ebert D, Koskella B, Poss M, Sadd BM. 2013 The Origin of Specificity by Means of Natural Selection: Evolved and Nonhost Resistance in Host–Pathogen Interactions. *Evolution* **67**, 1–9. (doi:10.1111/j.1558-5646.2012.01793.x)

12. Best A, White A, Kisdi É, Antonovics J, Brockhurst MA, Boots M. 2010 The Evolution of Host-Parasite Range. *Am. Nat.* **176**, 63–71. (doi:10.1086/653002)

547 13. Boots M, White A, Best A, Bowers R. 2014 How Specificity and Epidemiology Drive the
548 Coevolution of Static Trait Diversity in Hosts and Parasites. *Evolution* **68**, 1594–1606.
549 (doi:10.1111/evo.12393)

550 14. Jaenike J. 1978 A hypothesis to account for the maintenance of sex within populations. *Evol*
551 *Theory* **3**, 191–194.

552 15. Lively CM, Dybdahl MF. 2000 Parasite adaptation to locally common host genotypes. *Nature*
553 **405**, 679. (doi:10.1038/35015069)

554 16. Connell JH. 1971 On the role of natural enemies in preventing competitive exclusion in
555 some marine animals and in rain forest trees. *Dyn. Popul.* **298**, 312.

556 17. Janzen DH. 1970 Herbivores and the Number of Tree Species in Tropical Forests. *Am. Nat.*
557 **104**, 501–528. (doi:10.1086/282687)

558 18. Thompson JN. 2005 *The Geographic Mosaic of Coevolution*. University of Chicago Press.

559 19. Guth S, Visher E, Boots M, Brook CE. 2019 Host phylogenetic distance drives trends in virus
560 virulence and transmissibility across the animal–human interface. *Philos. Trans. R. Soc. B*
561 *Biol. Sci.* **374**, 20190296. (doi:10.1098/rstb.2019.0296)

562 20. Woolhouse MEJ, Gowtage-Sequeria S. 2005 Host Range and Emerging and Reemerging
563 Pathogens. *Emerg. Infect. Dis.* **11**, 1842–1847. (doi:10.3201/eid1112.050997)

564 21. Sexton JP, Montiel J, Shay JE, Stephens MR, Slatyer RA. 2017 Evolution of Ecological Niche
565 Breadth. *Annu. Rev. Ecol. Evol. Syst.* **48**, 183–206. (doi:10.1146/annurev-ecolsys-110316-
566 023003)

567 22. Stearns SC. 1989 Trade-Offs in Life-History Evolution. *Funct. Ecol.* **3**, 259–268.
568 (doi:10.2307/2389364)

569 23. Amado A, Campos PRA. 2019 Ecological specialization under multidimensional trade-offs.
570 *Evol. Ecol.* **33**, 769–789. (doi:10.1007/s10682-019-10013-4)

571 24. Cressler CE, King AA, Werner EE. 2010 Interactions between Behavioral and Life-History
572 Trade-Offs in the Evolution of Integrated Predator-Defense Plasticity. *Am. Nat.* **176**, 276–
573 288. (doi:10.1086/655425)

574 25. Steiner UK, Pfeiffer T. 2007 Optimizing Time and Resource Allocation Trade-Offs for
575 Investment into Morphological and Behavioral Defense. *Am. Nat.* **169**, 118–129.
576 (doi:10.1086/509939)

577 26. Regoes RR, Nowak MA, Bonhoeffer S. 2000 Evolution of Virulence in a Heterogeneous Host
578 Population. *Evolution* **54**, 64–71. (doi:10.1111/j.0014-3820.2000.tb00008.x)

579 27. Boots M, Sasaki A. 1999 'Small worlds' and the evolution of virulence: infection occurs
580 locally and at a distance. *Proc. R. Soc. B Biol. Sci.* **266**, 1933–1938.

581 28. Gandon S, Poulin R. 2004 Evolution of multihost parasites. *Evolution* **58**, 455–469.
582 (doi:10.1554/03-390)

583 29. Osnas EE, Dobson AP. 2012 Evolution of Virulence in Heterogeneous Host Communities
584 Under Multiple Trade-Offs. *Evolution* **66**, 391–401. (doi:10.1111/j.1558-5646.2011.01461.x)

585 30. Williams PD. 2012 New Insights into Virulence Evolution in Multigroup Hosts. *Am. Nat.* **179**,
586 228–239. (doi:10.1086/663690)

587 31. Berngruber TW, Lion S, Gandon S. 2015 Spatial Structure, Transmission Modes and the
588 Evolution of Viral Exploitation Strategies. *PLOS Pathog.* **11**, e1004810.
589 (doi:10.1371/journal.ppat.1004810)

590 32. Boots M, Sasaki A. 2000 The evolutionary dynamics of local infection and global
591 reproduction in host-parasite interactions. *Ecol. Lett.* **3**, 181–185.

592 33. Lion S, Boots M. 2010 Are parasites '"prudent"' in space? *Ecol. Lett.* **13**, 1245–1255.
593 (doi:10.1111/j.1461-0248.2010.01516.x)

594 34. Boots M, Mealor M. 2007 Local Interactions Select for Lower Pathogen Infectivity. *Science*
595 **315**, 1284–1286. (doi:10.1126/science.1137126)

596 35. Kerr B, Neuhauser C, Bohannan BJM, Dean AM. 2006 Local migration promotes competitive
597 restraint in a host–pathogen 'tragedy of the commons'. *Nature* **442**, 75–78.
598 (doi:10.1038/nature04864)

599 36. Elton CS. 1958 The ecology of invasions by animals and plants. *Ecol. Invasions Anim. Plants*

600 37. Visher E, Boots M. 2020 The problem of mediocre generalists: population genetics and eco-
601 evolutionary perspectives on host breadth evolution in pathogens. *Proc. R. Soc. B Biol. Sci.*
602 **287**, 20201230. (doi:10.1098/rspb.2020.1230)

603 38. Cornwall DH, Kubinak JL, Zachary E, Stark DL, Seipel D, Potts WK. 2018 Experimental
604 manipulation of population-level MHC diversity controls pathogen virulence evolution in
605 Mus musculus. *J. Evol. Biol.* **31**, 314–322. (doi:10.1111/jeb.13225)

606 39. Gibson AK. 2022 Genetic diversity and disease: The past, present, and future of an old idea.
607 *Evolution* **76**, 20–36. (doi:10.1111/evo.14395)

608 40. González R, Butković A, Elena SF. 2019 Role of host genetic diversity for susceptibility-to-
609 infection in the evolution of virulence of a plant virus. *Virus Evol.* **5**.
610 (doi:10.1093/ve/vez024)

611 41. Hughes WOH, Boomsma JJ. 2004 Genetic Diversity and Disease Resistance in Leaf-Cutting
612 Ant Societies. *Evolution* **58**, 1251–1260. (doi:10.1111/j.0014-3820.2004.tb01704.x)

613 42. Kubinak JL, Ruff JS, Hyzer CW, Slev PR, Potts WK. 2012 Experimental viral evolution to
614 specific host MHC genotypes reveals fitness and virulence trade-offs in alternative MHC
615 types. *Proc. Natl. Acad. Sci.* **109**, 3422–3427. (doi:10.1073/pnas.1112633109)

616 43. White PS, Choi A, Pandey R, Menezes A, Penley M, Gibson AK, de Roode J, Morran L. 2020
617 Host heterogeneity mitigates virulence evolution. *Biol. Lett.* **16**, 20190744.
618 (doi:10.1098/rsbl.2019.0744)

619 44. Bono LM, Draghi JA, Turner PE. 2019 Evolvability Costs of Niche Expansion. *Trends Genet.* **0**.
620 (doi:10.1016/j.tig.2019.10.003)

621 45. Bono LM, Smith LB, Pfennig DW, Burch CL. 2017 The emergence of performance trade-offs
622 during local adaptation: insights from experimental evolution. *Mol. Ecol.* **26**, 1720–1733.
623 (doi:10.1111/mec.13979)

624 46. Burmeister AR, Turner PE. 2020 Trading-off and trading-up in the world of bacteria–phage
625 evolution. *Curr. Biol.* **30**, R1120–R1124. (doi:10.1016/j.cub.2020.07.036)

626 47. Remold SK. 2012 Understanding specialism when the jack of all trades can be the master of
627 all. *Proc. R. Soc. B Biol. Sci.* **279**, 4861–4869. (doi:10.1098/rspb.2012.1990)

628 48. Whitlock MC. 1996 The Red Queen Beats the Jack-Of-All-Trades: The Limitations on the
629 Evolution of Phenotypic Plasticity and Niche Breadth. *Am. Nat.* **148**, S65–S77.

630 49. Anderson JT, Lee C-R, Rushworth CA, Colautti RI, Mitchell-Olds T. 2013 Genetic trade-offs
631 and conditional neutrality contribute to local adaptation. *Mol. Ecol.* **22**, 699–708.
632 (doi:10.1111/j.1365-294X.2012.05522.x)

633 50. Kawecki TJ, Ebert D. 2004 Conceptual issues in local adaptation. *Ecol. Lett.* **7**, 1225–1241.
634 (doi:10.1111/j.1461-0248.2004.00684.x)

635 51. Nuismer SL. 2006 Parasite Local Adaptation in a Geographic Mosaic. *Evolution* **60**, 24–30.

636 52. Gandon S. 2002 Local adaptation and the geometry of host–parasite coevolution. *Ecol. Lett.*
637 **5**, 246–256. (doi:10.1046/j.1461-0248.2002.00305.x)

638 53. Gandon S, Capowiez Y, Dubois Y, Michalakis Y, Olivieri I. 1996 Local adaptation and gene-
639 for-gene coevolution in a metapopulation model. *Proc R Soc Lond B* **263**, 1003–1009.
640 (doi:10.1098/rspb.1996.0148)

641 54. Gandon S, Michalakis Y. 2002 Local adaptation, evolutionary potential and host–parasite
642 coevolution: interactions between migration, mutation, population size and generation
643 time. *J. Evol. Biol.* **15**, 451–462. (doi:10.1046/j.1420-9101.2002.00402.x)

644 55. Gage MJ. 1995 Continuous variation in reproductive strategy as an adaptive response to
645 population density in the moth Plodia interpunctella. *Proc. R. Soc. Lond. B Biol. Sci.* **261**, 25–
646 30. (doi:10.1098/rspb.1995.0112)

647 56. Mohandass S, Arthur FH, Zhu KY, Throne JE. 2007 Biology and management of Plodia
648 interpunctella (Lepidoptera: Pyralidae) in stored products. *J. Stored Prod. Res.* **43**, 302–311.
649 (doi:10.1016/j.jspr.2006.08.002)

650 57. Consigli RA, Tweeten KA, Anderson DK, Bulla LA. 1983 Granulosis Viruses, with Emphasis on
651 the Gv of the Indian Meal Moth, Plodia interpunctella. In *Advances in Virus Research* (eds
652 MA Lauffer, K Maramorosch), pp. 141–173. Academic Press. (doi:10.1016/S0065-
653 3527(08)60723-X)

654 58. Harrison RL, Rowley DL, Funk CJ. 2016 The Complete Genome Sequence of Plodia
655 Interpunctella Granulovirus: Evidence for Horizontal Gene Transfer and Discovery of an
656 Unusual Inhibitor-of-Apoptosis Gene. *PLoS ONE* **11**, e0160389.
657 (doi:10.1371/journal.pone.0160389)

658 59. Tidbury H. 2012 The Evolutionary Ecology of Antiviral Resistance in Insects. phd, University
659 of Sheffield. See http://etheses.whiterose.ac.uk/2937/.

660 60. Begon M, Daud KBH, Young P, Howells RE. 1993 The Invasion and Replication of a
661 Granulosis Virus in the Indian Meal Moth, Plodia interpunctella: An Electron Microscope
662 Study. *J. Invertebr. Pathol.* **61**, 281–295. (doi:10.1006/jipa.1993.1053)

663 61. Visher E, Uricchio L, Bartlett L, DeNamur N, Yarcan A, Alhassani D, Boots M. 2022 The
664 evolution of host specialization in an insect pathogen. *Evolution* **76**, 2375–2388.
665 (doi:10.1111/evo.14594)

666 62. Bartlett LJ, Wilfert L, Boots M. 2018 A genotypic trade-off between constitutive resistance
667 to viral infection and host growth rate. *Evolution* **72**, 2749–2757. (doi:10.1111/evo.13623)

668 63. Bartlett LJ, Visher E, Haro Y, Roberts KE, Boots M. 2020 The target of selection matters: An
669 established resistance—development-time negative genetic trade-off is not found when
670 selecting on development time. *J. Evol. Biol.* **33**, 1109–1119. (doi:10.1111/jeb.13639)

671 64. Boots M, Childs D, Crossmore J, Tidbury H, Rudolf V. 2021 Experimental evidence that local
672 interactions select against selfish behaviour. *Ecol. Lett.* **24**, 1187–1192.
673 (doi:10.1111/ele.13734)

674 65. Boots M, Childs D, Reuman DC, Mealor M. 2009 Local Interactions Lead to Pathogen-Driven
675 Change to Host Population Dynamics. *Curr. Biol.* **19**, 1660–1664.
676 (doi:10.1016/j.cub.2009.07.070)

66. Oppert B, Hammel R, Throne JE, Kramer KJ. 2000 Fitness costs of resistance to Bacillus thuringiensis in the Indianmeal moth, Plodia interpunctella. *Entomol. Exp. Appl.* **96**, 281–287. (doi:10.1046/j.1570-7458.2000.00707.x)

67. Bolker BM, Brooks ME, Clark CJ, Geange SW, Poulsen JR, Stevens MHH, White J-SS. 2009 Generalized linear mixed models: a practical guide for ecology and evolution. *Trends Ecol. Evol.* **24**, 127–135. (doi:10.1016/j.tree.2008.10.008)

68. R Core Team. 2021 *R: A language and environment for statistical computing.* Vienna, Austria: R Foundation for Statistical Computing. See https://www.r-project.org/.

69. Bates D, Mächler M, Bolker B, Walker S. 2015 Fitting Linear Mixed-Effects Models Using lme4. *J. Stat. Softw.* **67**, 1–48. (doi:10.18637/jss.v067.i01)

70. Brooks ME, Kristensen K, Benthem KJ van, Magnusson A, Berg CW, Nielsen A, Skaug HJ, Mächler M, Bolker BM. 2017 glmmTMB Balances Speed and Flexibility Among Packages for Zero-inflated Generalized Linear Mixed Modeling. *R J.* **9**, 378–400.

71. Fox J, Weisberg S. 2019 *An R Companion to Applied Regression, 3rd Edition*. See https://socialsciences.mcmaster.ca/jfox/Books/Companion/index.html.

72. Hartig F, Lohse L. 2021 DHARMa: Residual Diagnostics for Hierarchical (Multi-Level / Mixed) Regression Models.

73. Lenth RV, Buerkner P, Herve M, Love J, Miguez F, Riebl H, Singmann H. 2022 emmeans: Estimated Marginal Means, aka Least-Squares Means.

74. Pedersen TL. 2020 patchwork: The Composer of Plots.

75. Singmann H *et al.* 2019 afex: Analysis of Factorial Experiments.

76. Wickham H. 2009 *ggplot2 - Elegant Graphics for Data Analysis*. Springer. See https://www.springer.com/gp/book/9780387981413.

77. Wickham H *et al.* 2019 Welcome to the Tidyverse. *J. Open Source Softw.* **4**, 1686. (doi:10.21105/joss.01686)

78. Harrison XA. 2014 Using observation-level random effects to model overdispersion in count data in ecology and evolution. *PeerJ* **2**, e616. (doi:10.7717/peerj.616)

79. Abrams PA. 2006 The Prerequisites for and Likelihood of Generalist-Specialist Coexistence. *Am. Nat.* **167**, 329–342. (doi:10.1086/499382)

80. Gibson AK, White PS, Penley MJ, de Roode JC, Morran LT. 2020 An experimental test of parasite adaptation to common versus rare host genotypes. *Biol. Lett.* **16**, 20200210. (doi:10.1098/rsbl.2020.0210)

81. Dybdahl MF, Storfer A. 2003 Parasite local adaptation: Red Queen versus Suicide King. *Trends Ecol. Evol.* **18**, 523–530. (doi:10.1016/S0169-5347(03)00223-4)

82. Lion S, Metz JAJ. 2018 Beyond R0 Maximisation: On Pathogen Evolution and Environmental Dimensions. *Trends Ecol. Evol.* **33**, 458–473. (doi:10.1016/j.tree.2018.02.004)

83. Plowright RK, Parrish CR, McCallum H, Hudson PJ, Ko AI, Graham AL, Lloyd-Smith JO. 2017 Pathways to zoonotic spillover. *Nat. Rev. Microbiol.* **15**, 502–510. (doi:10.1038/nrmicro.2017.45)

84. Guth S, Mollentze N, Renault K, Streicker DG, Visher E, Boots M, Brook CE. 2022 Bats host the most virulent—but not the most dangerous—zoonotic viruses. *Proc. Natl. Acad. Sci.* **119**, e2113628119. (doi:10.1073/pnas.2113628119)

85. Tompkins DM, White AR, Boots M. 2003 Ecological replacement of native red squirrels by invasive greys driven by disease. *Ecol. Lett.* **6**, 189–196. (doi:10.1046/j.1461-0248.2003.00417.x)

86. Greischar MA, Koskella B. 2007 A synthesis of experimental work on parasite local adaptation. *Ecol. Lett.* **10**, 418–434. (doi:10.1111/j.1461-0248.2007.01028.x)

87. Bisschop K, Blankers T, Mariën J, Wortel MT, Egas M, Groot AT, Visser ME, Ellers J. 2022 Population bottleneck has only marginal effect on fitness evolution and its repeatability in dioecious Caenorhabditis elegans. *Evolution* **n/a**. (doi:10.1111/evo.14556)

88. Boots M, Begon M. 1993 Trade-Offs with Resistance to a Granulosis Virus in the Indian Meal Moth, Examined by a Laboratory Evolution Experiment. *Funct. Ecol.* **7**, 528–534. (doi:10.2307/2390128)